5-2022

Evaluating sex-dependent changes in the gut microbiome caused by Polychlorinated Biphenyl (PCB) exposure.

Zayna Qaissi
University of Louisville

EVALUATING SEX-DEPENDENT CHANGES IN THE GUT MICROBIOME CAUSED BY POLYCHLORINATED BIPHENYL (PCB) EXPOSURE

By

Zayna H. Qaissi

Thesis Submitted in partial fulfillment of the requirements

for Graduation summa cum laude

and

for Graduation with Honors from the Department of Biology and

The College of Arts and Sciences

University of Louisville

Spring 2022

EVALUATING SEX-DEPENDENT CHANGES IN THE GUT MICROBIOME CAUSED BY POLYCHLORINATED BIPHENYL (PCB) EXPOSURE

By

Zayna H. Qaissi

Thesis Approved March 2022

By the following Thesis Committee:

Banrida Wahlang, Ph.D. (Mentor)

Cynthia Corbitt, Ph.D.

Mathew Cave, M.D.

TABLE OF CONTENTS

PAGE

ABSTRACT

Polychlorinated biphenyls (PCBs) are persistent organic pollutants that have been associated with fatty liver disease, cardiovascular diseases, and other metabolic dysfunctions. Our laboratory group previously demonstrated that exposures to PCBs led to sex-dependent liver outcomes with female mice showing higher susceptibility to PCB-induced liver toxicity. Some of the underlying mechanisms driving these sex-dependent outcomes that were identified included PCB-modulated endocrine disruption. However, the PCB effects on the gut microbiome and the gut liver axis have not been investigated. Therefore, the objective of the current study is to identify PCB-induced changes in the gut microbiome and identify if this could be a cause for the observed sex-dependent PCB toxicity. Male and female C57BL6 mice were exposed to a mixture of PCBs for two weeks; cecal and ileal samples were isolated at euthanasia. 16S sequencing was performed and RT-PCR was used to examine ileal gene expression. The metagenomics results demonstrated significant sex differences in bacterial composition with PCB-exposed female mice exhibiting the lowest alpha diversity. In terms of beta diversity, there was a predominant sex effect driving the differences while PCB effects were subtler in both sexes. Additionally, assessment of ileal gene expression demonstrated that the PCB-exposed female mice had lower expression for genes encoding gut barrier proteins, namely *Cldn2* and *Muc2*. With regards to inflammatory responses, PCB-exposed female mice showed decreased gene expression for the antimicrobial peptide, namely *Tff3*, thereby implicating an unhealthy mucosal environment. Taken together, the results demonstrated that PCB exposure impacted the gut microbiome and gut function in a sex-dependent manner, thus confirming the existence of sex differences on gut microbiota

with environmental exposures. Future studies will include identification of key bacterial phyla that were altered with sex and exposure and correlating them with hepatic toxicity endpoints.

LAY SUMMARY

Polychlorinated biphenyls (PCBs) are hazardous substances found in the environment that have been linked to a variety of health problems in people who are exposed to them. Liver disease, reproductive abnormalities, and cardiovascular illnesses are among the health consequences. While extensive studies have been done using experimental models to investigate PCB-mediated organ damage and toxicity, little is known about how PCBs behave in terms of their harmful effects in the context of sex and gender. The goal of the proposed study is to understand how pollutants like PCBs can alter the composition of gut bacteria, how these changes affect liver health, and whether these changes are different in males and females. This research will help us determine the association between different environmental pollutants with sex and gender, as well as identify if men or women are more susceptible to PCB-related health effects.

INTRODUCTION

Background

Polychlorinated biphenyls (PCBs) are halogenated aromatic hydrocarbons belonging to the class of persistent organic pollutants. PCBs are also known as “forever chemicals” because they are resistant to metabolism and biodegradation. PCB exposures in humans have been associated with numerous diseases such as cancer, cardiovascular complications, diabetes and liver disease (1). Due to their thermodynamic stability, they were used as dielectric fluids in voltage transformers (capacitors) and other industrial applications. In 1979, PCB production and use were banned in the US by Congress (Toxic Substance Control Act). Despite being banned in the U.S. since the 1970s, PCBs were still used world-wide, and their production and use were globally banned at the Stockholm Convention in 2001. PCBs are still present in our environment and ecosystem due to their resistance to biodegradation. The primary method of human exposure is through PCB-laden food; due to the lipophilic nature of PCBs, they eventually bioaccumulate in adipose tissue. Hence, they continue to be a risk to both wildlife and human health.

The structural composition of PCBs is typically chlorination on the biphenyl ring, leading to coplanar and non-coplanar compounds, depending on the type of chlorine substitution (2). Coplanar compounds are classified as “dioxin-like” as they are able to activate the aryl hydrocarbon receptor (AhR), similar to the well-known chemical dioxin; coplanar PCBs consist of low-molecular weight congeners. Non-coplanar congeners are classified as “phenobarbital-like” or “non-dioxin-like” due to their ability to activate constitutive androstane receptor (CAR); non-coplanar PCBs consist of high molecular weight congeners. The Monsanto Corporation which was the primary company that

produced PCBs in North America at its plant in Anniston, AL, commercially sold PCBs as mixtures of congeners under the brand name “Aroclors”. The first-generation PCB commercial mixture, known as Aroclor 1260, consisted of 60% chlorine by weight. However, due to its toxic effects, it was replaced by second-generation PCB mixtures such as Aroclor 1016, with a lower chlorine content. Nevertheless, because Aroclor 1260 is highly chlorinated and is comprised of many high molecular weight congeners, it is resistant to metabolism, leading to bioaccumulation. The use of Aroclor 1260 is relevant in our research because it mimics current PCB bioaccumulation patterns in humans.

PCBs exposures are associated with many diseases including non-alcoholic fatty liver disease (NAFLD) and toxicant associated steatohepatitis (TASH) (3, 4). NAFLD is fatty liver disease characterized by lipid accumulation in the liver or steatosis and accompanied by inflammation (steatohepatitis). TASH is a form of NAFLD that is caused by exposure to chemical pollutants or toxicants such as PCBs (5). Previous studies have also reported liver disease prevalence within a known PCB-exposed population that resided in Anniston, AL and this study population was named the Anniston Community Health Survey (ACHS) population (6). In addition, experimental toxicology studies examining the role of PCBs in liver diseases have also indicated the existence of sex-dependent effects where female mice were more susceptible to PCB-induced TASH (7). Mechanistically, PCBs are thought to exacerbate their toxic effects on the liver, in part, through activation of CAR and pregnane-xenobiotic receptor (PXR), which are xenobiotic receptors that function to detoxify drugs and foreign chemicals in the liver through the activation of cytochrome P450s (8). These receptors play other roles in energy metabolism, steatosis and regulating the gut microbiota.

Recent studies have indicated that PCB exposure also caused gut microbiome alterations which could potentially play a role in TASH (9, 10). However, little is known about PCB effects on gut microbiome especially with low-dose, environmental exposures. Also, the existence of sex differences in PCB-induced altered gut microbiome has not been thoroughly studied. Therefore, the objective of the current study is to evaluate changes in gut microbiome caused by toxicant exposures, namely polychlorinated biphenyls (PCBs), and to identify the underlying sex differences.

We expected to observe differences in gut microbiota composition between male and female mice in parameters such as alpha and beta diversity. We also expected PCB exposures to change gut microbiota composition as well as gene expression of ileal permeability and function markers such as tight junction proteins. Based on our previous studies on liver endpoints, where PCB-exposed female mice were most susceptible to fatty liver disease, we expected that there will be an interaction between sex and exposure, wherein female mice have higher levels of microbiome alterations. Additionally, we expected PCB-exposed female mice to have lower gene expression levels of ileal barrier markers and higher level of inflammatory markers. Furthermore, the findings from our project will help identify and address research gaps in environmental health sciences pertaining to sex differences in PCB-induced altered gut microbiome.

Hypothesis

The central hypothesis of the current study is that exposures to environmental toxicants such as PCBs can cause alterations in gut microbiome composition and ileal

gene expression; furthermore, the effects of PCBs on gut microbiota differ between sexes.

MATERIALS AND METHODS

Animal Experimental Design

The animal study has already been performed by Wahlang et al (7). Briefly male and female mice (n =10) were exposed to either corn oil (vehicle control) or a PCB mix that was comprised of the commercial PCB mixture, Aroclor 1260 (20 mg/kg) and PCB126 (20 μg/kg) for 2 weeks. The PCB mix was administered via oral gavage. At the end of the study, mice were euthanized and tissues such as the liver, intestine and cecum were harvested. The animal protocol was approved by the University of Louisville Institutional Animal Care and Use Committee.

Bacterial DNA isolation

Microbial genomic DNA from cecal samples was isolated using the DNeasy Power Soil Pro Kit (Qiagen, Germantown, MD, USA) and instructions were followed according to the manufacturer's manual. Approximately 200 mg of cecal sample was added to Powerbead Pro tubes containing beads and CD 1 (Lysis Buffer) solution. The tubes were then vortexed and centrifuged. The supernatant was transferred to a 2 mL microcentrifuge tube and 200 μL of cold (8 °C) CD2 (inhibitor removal) solution was added. The solution was then vortexed, centrifuged and the supernatant was transferred to a new 2 mL microcentrifuge tube. 600 μL of CD3 (Binding Buffer) solution was added to the supernatant solution and vortexed. 650 μL of this lysate was then added to an MB spin column, and it was centrifuged. Flow-through was discarded and this step was repeated. The MB spin column was then placed into a clean 2 mL collection tube. It was washed by EA and C5 (wash) solution, respectively. The MB spin column was the placed into a new

a 1.5 mL elution tube. 50-100 μL of C6 (elution buffer) solution was then added near the white filter membrane and lastly, the solution was centrifuged, while the MB spin column was discarded.

16S Metagenomic Sequencing Library Preparation and Sequencing Run

The cecal microbiota was analyzed using the Illumina MiSqeq technology, focusing on V3 and V4 of 16S ribosomal RNA. Libraries were prepared using the Illuminas 16S library preparation guide and Illumina's Nextera Index Kit (FC-121-1012). Initially, the isolated microbial genomic DNA was quantified using the Quibot Broad Range (BR) Assay in a Quibot 2.0 Fluorometer. Amplicon PCR was carried out to amplify the 16S variable region of the genomic DNA using primers and overhang adaptors. Amplicon PCR was cleaned up using AMPure XP beads. Index PCR was then performed to attach dual indices and Illumina sequencing adapters using the Nextera XT Kit (FC-121-1012). Clean-up was then repeated. Sequencing libraries were then aliquoted and mixed to generate pooled libraries and a Bioanalyzer was used to quantify DNA amount. The genomic DNA library was then denatured and combined with the PhiX control library. Using a Nano-300 cycle test chip (MS-103-1001), sequencing was then performed to confirm sample concentrations followed by Illumina MiSeq Reagents Kit v3 (600 cycles) (MS-12-3003) at 9 pM and 30% PhIX.

Microbiome Sequencing Data Analysis

Quality control of the raw sequence data was carried out using FastQC (version 0.10.1). The sequence data were then trimmed and further analyzed using Quantitative

Insights into Microbial Ecology (QIIME 2) (version 2019.4). A tree was generated for phylogenetic diversity analyses using the representative sequences and core diversity analyses including alpha and beta diversity were performed. Algorithms used to measure alpha diversity were Shannon Index, observed_species (OTUs) and Faith_pd; algorithms used to measure beta diversity included UniFrac and Jaccard. The Emperor tool was used to explore the principal covariant analysis plot in the context of sample metadata which is the distance between samples (beta diversity) using weighted and unweighted UniFrac.

Gene expression analysis

RNA isolation, quantification and cDNA synthesis were performed on ileal samples (n = 10) that have been isolated from mice using previously described methods (3). RT-PCR was performed on the CFX384 TM Real-Time System (Biorad, Hercules, CA, USA) using iTaq Universal Probes Supermix and TaqMan probes (Biorad, Hercules, CA, USA). Gene expression levels were calculated according to the $2^{-\Delta\Delta Ct}$ method (11). The levels of mRNA were normalized relative to the levels of housekeeping genes and mean expression levels in unexposed, male mice was set at 1. The primers that were evaluated included *i)* genes encoding proteins involved in gut barrier integrity and function, namely, Tight Junction Protein 1 (TJP1), Claudin 1, Claudin 2, Occludin, Vascular Endothelial (VE) Cadherin (5), Mucin 1 (MUC1), Mucin 2 (MUC2), Fibroblast growth factor 15 (FGF15); and *ii)* genes involved in inflammation, namely ileal Trefoil factor 3 (TFF3), Interleukin 6 (IL-6), Interleukin 10 (IL-10), Tumor necrosis factor alpha (TNFα) and Transforming growth factor beta (TGF-β).

Statistical Analyses for Sequence Data

Kruskal-Wallis test was used for pairwise comparisons between all experimental groups for core metric analysis, and an FDR adjusted *p*-value (q-value) was used to infer significance (*p*-value <0.05). For principal covariant analysis, the mean distance between two groups was compared using multivariate analysis of variance (PERMANOVA), and nonparametric *p*-values were calculated using 999 Monte Carlo permutations.

Statistical Analyses for RT-PCR results

Statistical comparisons were performed using GraphPad Prism version 9 (GraphPad Software Inc., La Jolla, CA). The gene expression data was analyzed via a Two-Way ANOVA, for two factors, namely “Sex” and “PCBs” and their interactions. For the ANOVA analysis, *p*-value <0.05 was considered statistically significant. Due to the exploratory nature of the study, sub-group analyses for multiple comparisons were also performed within the male and female groups (CON *vs.* PCB) using a *t*-test (*p*-value <0.05).

RESULTS

Alpha Diversity

Alpha diversity which represents the array of species within the designated samples, was measured using QIIME metrics, specifically observed_species (OTUs – observed taxonomical units), Faith_pd tree, and Shannon Index measurements. Box plots graphically illustrating the number of species were plotted and these are represented in Figures 1A (Shannon), 1B (OTUs), and 1C (Faith_pd). With the Shannon Index metric, which considers species richness and abundance, there was a significant difference between the PCB-exposed male group (M-PCB) in comparison to the female control group (F-CON). However, with the observed_species (OTU) metric, which accounts only for species abundance, there was a significant difference between the male (M-PCB) and female (F-PCB) groups with PCB exposure. Importantly, for the OTUs metric, the PCB-exposed female group displayed the lowest microbial alpha diversity among all the groups. Finally, for the Faith_pd metric, which measures phylogenetic differences among species, there were no significant differences between the groups.

Alpha Diversity

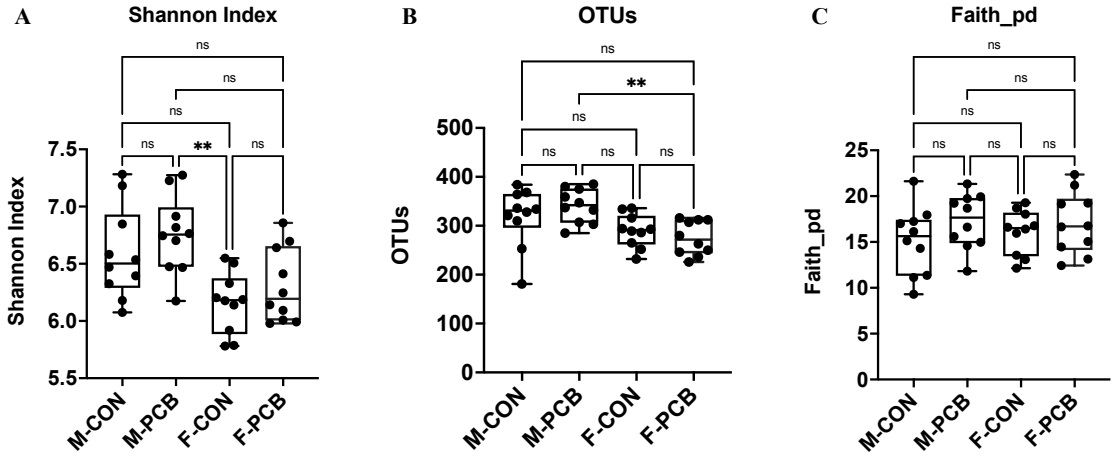

Figure 1. Effects of PCB exposure on alpha diversity in male and female mice. Alpha diversity was measured using three QIIME metrics, namely A) Shannon Index, B) observed_species (OTUs), and C) Faith_pd. Kruskal-Wallis test was performed for pairwise comparison between different groups for faith_pd. *q*-value <0.05 denotes statistical significance in bacterial diversity between the two groups.

Beta Diversity

Beta diversity was computed to compare how each group of samples differed relative to other samples analyzed. Both unweighted and weighted variants of UniFrac were used to measure the distance between the pairs of samples. Unweighted UniFrac accounts for presence or absence of taxa across individual systems. In contrast, weighted UniFrac takes into account the abundance of each taxa across individual samples in addition to the absence or presence of taxa. In addition, Jaccard algorithm, which measures similarity of bacterial composition between samples, was also employed to measure beta diversity. The matrix for both weighted and unweighted UniFrac as well as Jaccard was visualized using the principle co-variant analyses (PCA). The plots resulted in three PCA coordinates, namely axis 1, 2 and 3. This is a 3-dimensional representation of the acquired data as represented in Figure 2A, Figure 3A and Figure 4A. Results from the PERMANOVA analysis, which compared significance differences between groups, are represented in Figure 2B, Figure 3B and Figure 4B.

According to the weighted and unweighted UniFrac results, there was a significant difference in beta diversity that resulted from both sex and PCB exposure effects. Firstly, there was a difference between the males and females for the unweighted (q-value=0.008) and weighted (q-value=0.006) results. There was also a significant difference between the males and females, with PCB exposure, for both unweighted (q-value=0.003) and weighted (q-value=0.044) results. Significant differences were observed across all groups with Jaccard.

A. Beta Diversity – Unweighted UniFrac (With Ellipse)

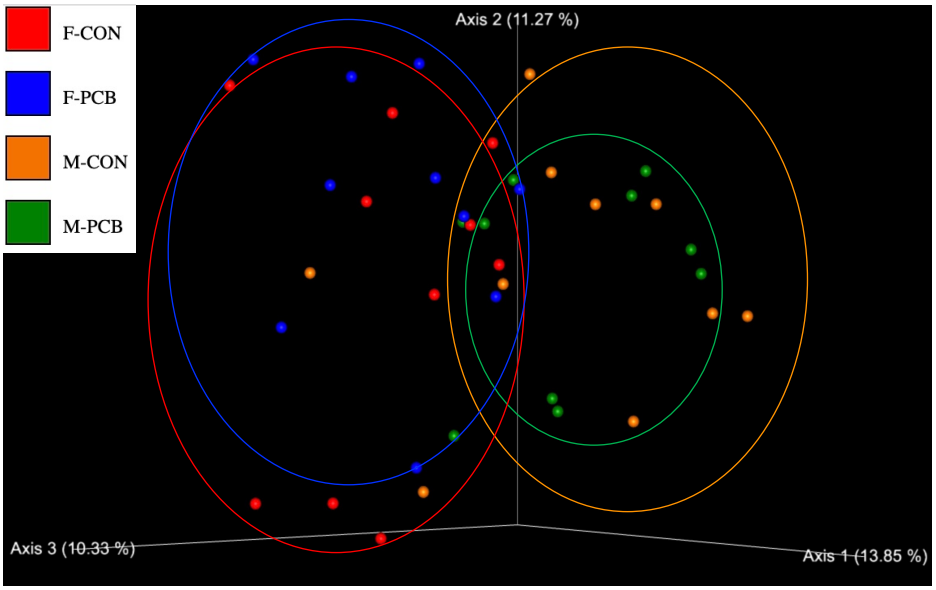

B. PERMANOVA Analysis for Unweighted UniFrac

Comparisons		q-value
Group 1	Group 2	
F-CON	F-PCB	0.124
F-CON	M-CON	0.008
F-CON	M-PCB	0.003
F-PCB	M-CON	0.009
F-PCB	M-PCB	0.003
M-CON	M-PCB	0.038

Figure 2. Effects of PCB exposure on beta diversity in male and female mice. A) Beta diversity was computed by measuring distance between pairs of samples using unweighted variant of UniFrac and matrix visualized with principal covariant analysis. B) Table depicting results obtained from the PERMANOVA pairwise test. *q*-value <0.05 denotes statistical significance in bacterial diversity between the two groups.

A. Beta Diversity – Weighted UniFrac (With Ellipse)

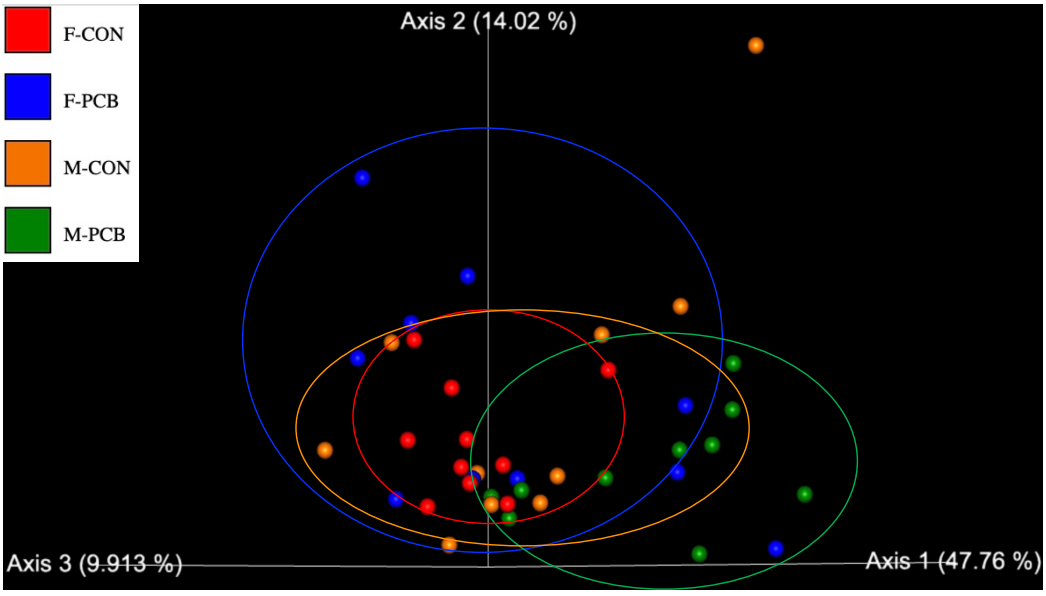

B. PERMANOVA Analysis for Weighted UniFrac

Comparisons		q-value
Group 1	Group 2	
F-CON	F-PCB	0.112
F-CON	M-CON	0.006
F-CON	M-PCB	0.006
F-PCB	M-CON	0.112
F-PCB	M-PCB	0.044
M-CON	M-PCB	0.112

Figure 3. Effects of PCB exposure on beta diversity in male and female mice. A) Beta diversity was computed by measuring distance between pairs of samples using weighted variant of UniFrac and matrix visualized with principal covariant analysis. B) Table depicting results obtained from the PERMANOVA pairwise test. *q*-value <0.05 denotes statistical significance in bacterial diversity between the two groups.

A. Beta Diversity – Jaccard (With Ellipse)

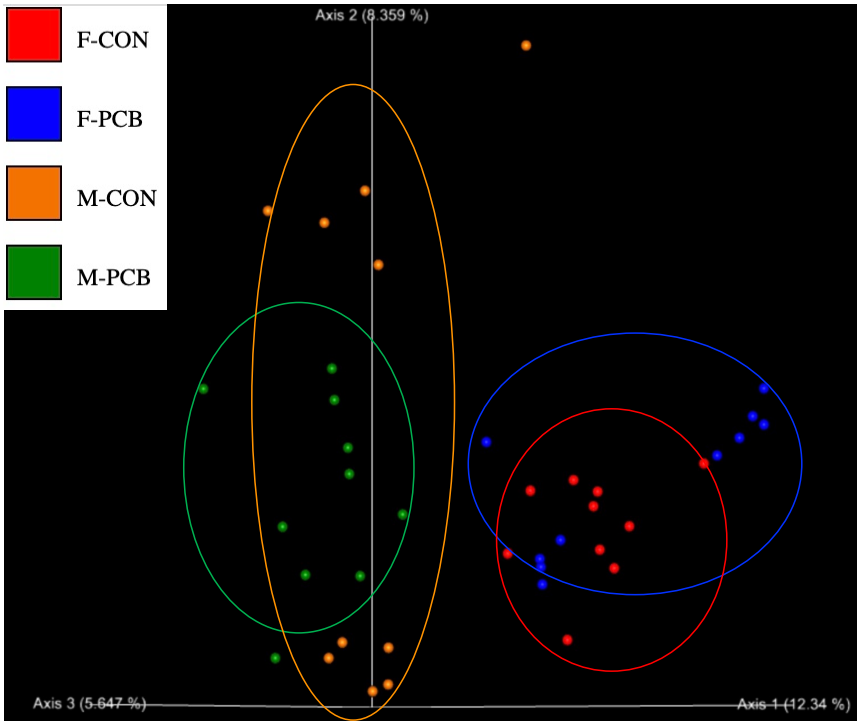

B. PERMANOVA Analysis for Jaccard

Comparisons		q-value
Group 1	Group 2	
F-CON	F-PCB	0.002
F-CON	M-CON	0.002
F-CON	M-PCB	0.002
F-PCB	M-CON	0.002
F-PCB	M-PCB	0.002
M-CON	M-PCB	0.017

Figure 4. Effects of PCB exposure on beta diversity in male and female mice. A) Beta diversity was computed using the Jaccard algorithm which measures the similarities between the samples. B) Table depicting results obtained from the PERMANOVA pairwise test. *q*-value <0.05 denotes statistical significance in bacterial diversity between the two groups.

Hepatic Gene Expression

To further investigate the impact of PCB exposure on gut function within the female and male groups, and to further identify if the gut barrier properties were affected due to the altered microbiome, specific ileal markers of gut permeability and function were assessed. The ileum was specifically chosen for this study because it is the most immunologically active area of the gut and has a high sensitivity to alterations in barrier function (12). Ileal mRNA levels of tight junction protein 1 (*Tjp1*) was initially examined. *Tjp1* is the gene encoding for zonula occludens-1, a scaffolding protein that connects tight junction trans-membrane proteins like claudins (*Cldn1,2*) and occludin (*Ocln*) to the actin cytoskeleton (13). Our RT-PCR results demonstrated there were no significant differences in *Tjp1* mRNA levels (Figure 5A). Further analysis of other gut barrier proteins demonstrated that PCB exposure decreased both *Cldn1* and *Cldn2* mRNA levels (Figures 5B and 5C). Compared to their respective baseline groups, PCB-exposed male mice did not show significant differences for either *Cldn1* or *Cldn2*; however, there was a significant decrease in *Cldn1* expression in the PCB-exposed female group compared to their unexposed female counterparts. Similar to *Cldn2*, there was a decrease in *Ocln* gene expression with PCB exposure in the female group (Figure 5D). Precedingly, we examined the adhesion molecule vascular endothelial cadherin-5 (*Chd5*), and mucus gel-forming proteins Mucin 1 and 2 (*Muc1* and *Muc*2). There were no observed differences between the control and exposed groups for *Cdh5* (Figure 5E) for either males or females. However, there was a non-significant trend (*p*-value=0.0778) for decreased *Muc1* expression with PCB exposure (Figure 5F); furthermore, sub-group analysis revealed that the PCB-exposed female mice also showed a non-significant trend for decreased *Muc1*

expression (p-value=0.067). In terms of *Muc2*, the PCB-exposed female group showed significantly lower expression levels (Figure 5G).

Additionally, we examined expression levels of intestinal antimicrobial factors, specifically Trefoil Factor 3 (*Tff3*) (Figure 6A), and mucosal inflammatory markers and cytokines, namely tumor necrosis factor alpha (*Tnfa*), transforming growth factor beta (*Tgfb*), interleukin 6 (*Il-6*) and interleukin 10 (*Il-10*) (Figure 6B - 6E). While there was a PCB effect for decreased *Tff3* expression, there were however no significant differences for the other cytokines and markers. Interestingly, sub-group analysis demonstrated that the PCB-exposed female mice showed a non-significant trend for decreased *IL-6* gene expression (*p*-value=0.0755).

Lastly, the hepatic expression of the gene encoding *Fgf-15* was evaluated. *Fgf-15* is a fibroblast growth factor secreted by intestinal epithelial cells and aids in hepatocyte growth, bile acid homeostasis, as well regulating levels of glucose and lipid metabolism (14). There was a sex-dependent effect for *Fgf15* gene expression with female mice having higher expression levels (Figure 6F). However, there was no reported PCB effect.

A

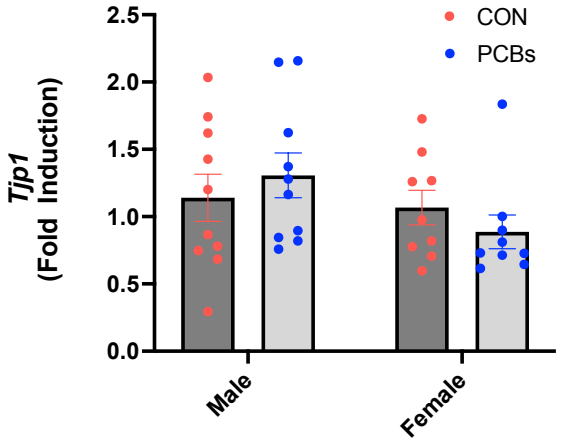

Source of Variation	% of total variation	P value	P value summary
Interaction	3.410	0.2638	ns
Sex	6.806	0.1177	ns
PCBs	0.005868	0.9627	ns

B

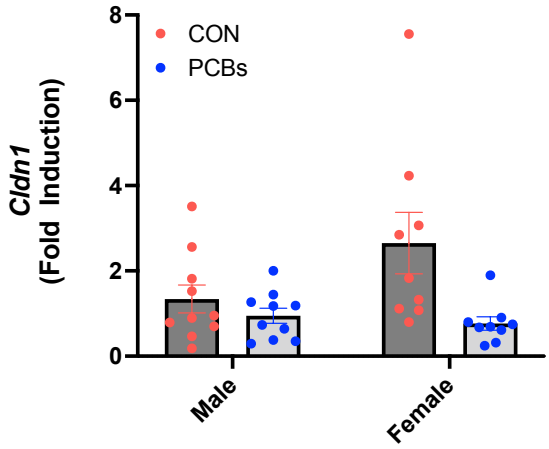

Source of Variation	% of total variation	P value	P value summary
Interaction	7.375	0.0713	ns
Sex	4.215	0.1684	ns
PCBs	17.19	0.0075	**

C

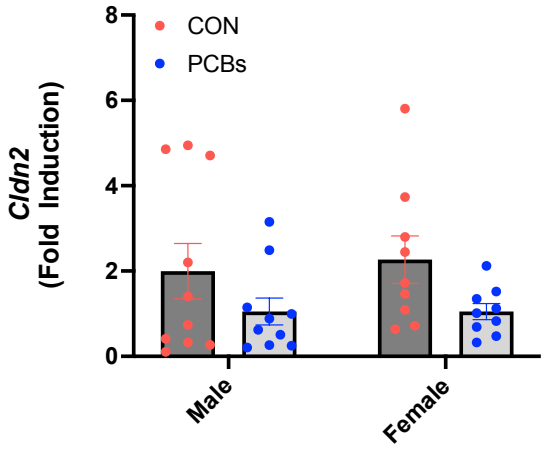

Source of Variation	% of total variation	P value	P value summary
Interaction	0.2104	0.7753	ns
Sex	0.2049	0.7782	ns
PCBs	13.31	0.0284	*

D

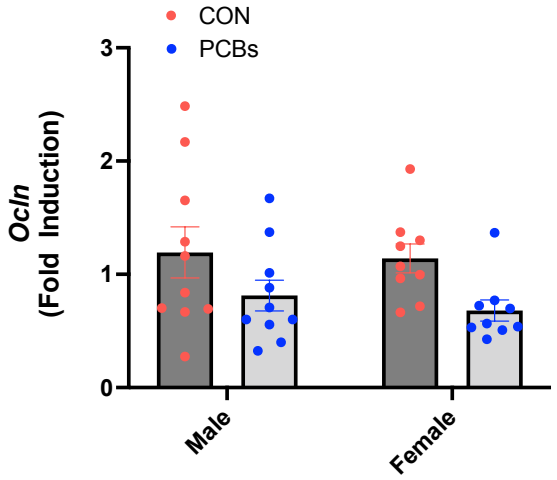

Source of Variation	% of total variation	P value	P value summary
Interaction	0.1519	0.8035	ns
Sex	0.8215	0.5635	ns
PCBs	17.07	0.0119	*

E

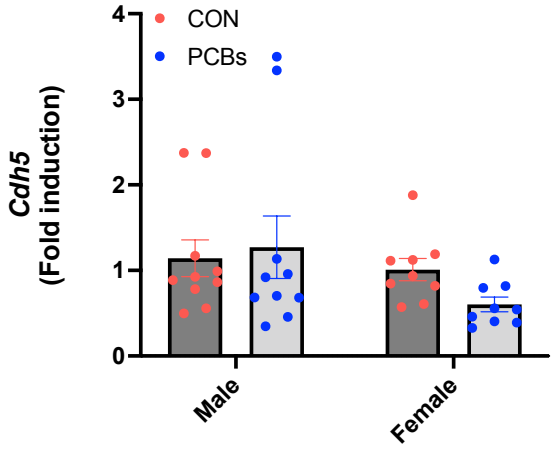

Source of Variation	% of total variation	P value	P value summary
Interaction	3.372	0.2627	ns
Sex	7.511	0.0983	ns
PCBs	0.8929	0.5617	ns

F

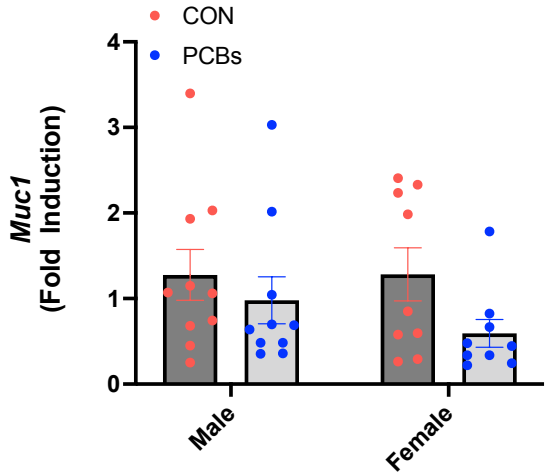

Source of Variation	% of total variation	P value	P value summary
Interaction	1.367	0.4749	ns
Sex	1.293	0.4870	ns
PCBs	8.660	0.0778	ns

G

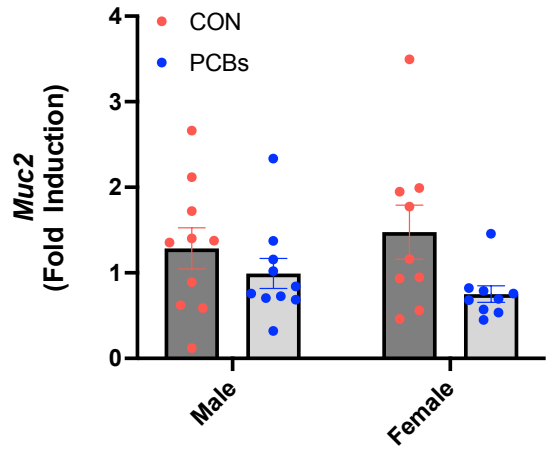

Source of Variation	% of total variation	P value	P value summary
Interaction	2.352	0.3389	ns
Sex	0.03359	0.9084	ns
PCBs	13.14	0.0282	*

Figure 5. Effects of sex and PCB exposure on ileal permeability markers. Ileal mRNA levels for genes encoding proteins involved in maintenance of barrier integrity and intestinal inflammation/function including (A) *Tjp1*, (B) *Cldn1*, (C) *Cldn2*, (D) *Ocln*, (E) *Cdh5*, (F) *Muc1*, and (G) *Muc2* were measured using RT- PCR. Values were normalized to male control mice (M-CON) and presented as mean ± SEM, $p < 0.05$. An ANOVA table with 2-way statistics are also presented

A

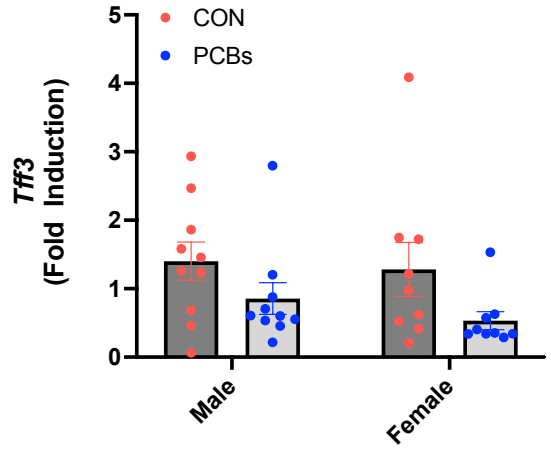

Source of Variation	% of total variation	P value	P value summary
Interaction	0.3313	0.7172	ns
Sex	1.621	0.4248	ns
PCBs	13.77	0.0244	*

B

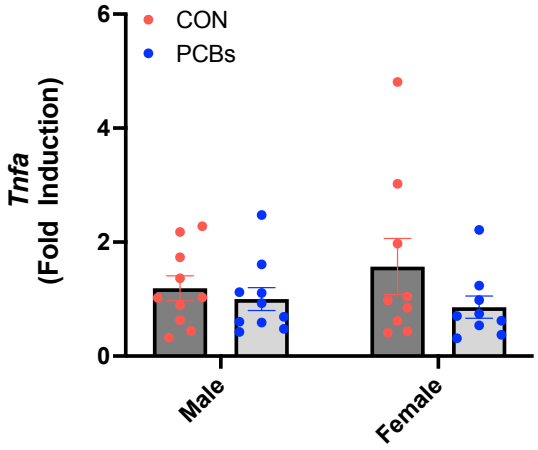

Source of Variation	% of total variation	P value	P value summary
Interaction	2.126	0.3804	ns
Sex	0.4378	0.6893	ns
PCBs	6.267	0.1363	ns

C

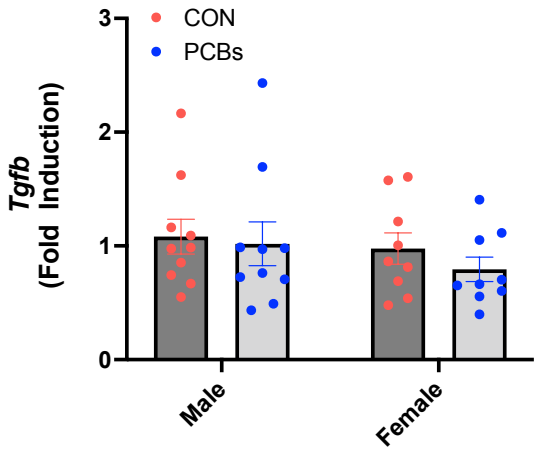

Source of Variation	% of total variation	P value	P value summary
Interaction	0.4143	0.7022	ns
Sex	3.175	0.2932	ns
PCBs	1.774	0.4304	ns

D

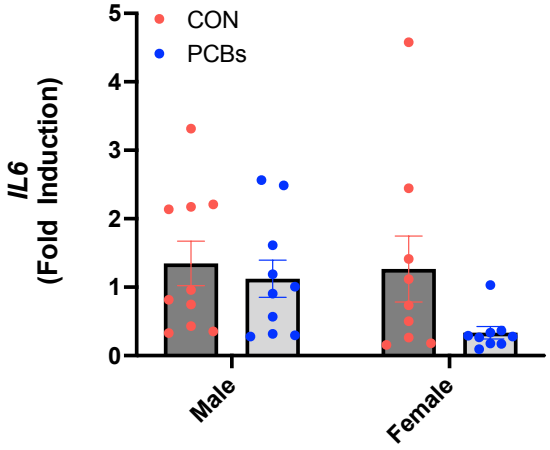

Source of Variation	% of total variation	P value	P value summary
Interaction	3.003	0.2806	ns
Sex	4.543	0.1863	ns
PCBs	8.030	0.0819	ns

E

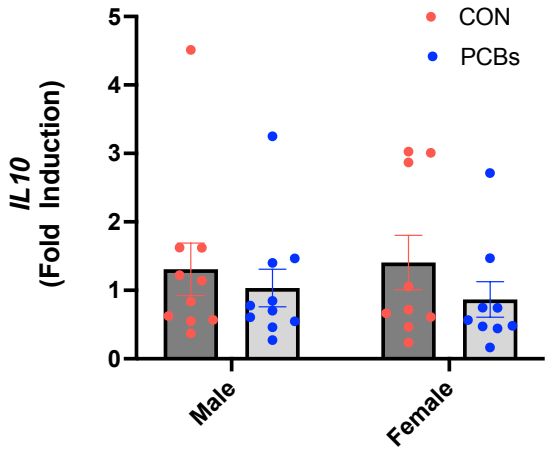

Source of Variation	% of total variation	P value	P value summary
Interaction	0.4388	0.6952	ns
Sex	0.02840	0.9205	ns
PCBs	4.130	0.2338	ns

F

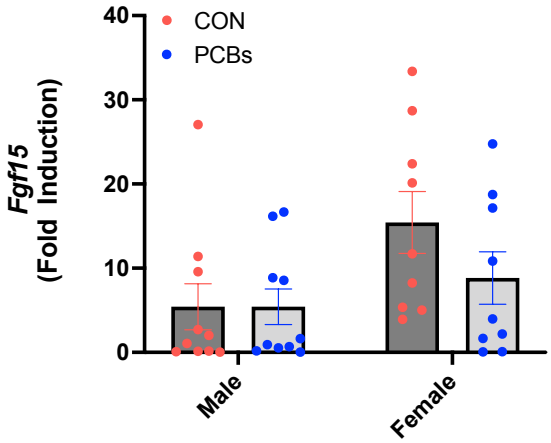

Source of Variation	% of total variation	P value	P value summary
Interaction	3.065	0.2662	ns
Sex	12.65	0.0279	*
PCBs	3.053	0.2671	ns

Figure 6. Effects of sex and PCB exposure on ileal inflammatory markers and function. Ileal mRNA levels for genes encoding proteins involved in maintenance of intestinal inflammation and function including (A) *Tff3*, (B) *Il6*, (C) *Il10* and (D) *Fgf15* were measured using RT-PCR. Values were normalized to male control mice (M-CON) and presented as mean ± SEM, $p < 0.05$. An ANOVA table with 2-way statistics are also presented.

DISCUSSION

The underlying mechanisms of toxicity caused by PCBs in the liver have been studied thoroughly, with main mechanisms being associated with activation of hepatic receptors, such as AhR, CAR and PXR (4). Nevertheless, there are additional mechanisms recently reported that include epigenetic modifications, molecular signaling disruption and microbiome alterations that still warrant further investigation. Importantly, the impact of PCB exposures on the relationship between the liver and gut microbiome is still largely understudied.

The gut-liver axis refers to the relationship between the gut and its microbiota, and the liver, due to integration of signals directed by dietary, genetic, and environmental factors. This interaction is founded by the portal vein, which provides access for gut-derived product to the liver while the liver feedback route provides access to the bile and antibody secretions to the intestine. Particularly, the interaction between the gut and liver depends on the mucosal and vascular barrier of the intestine, also known as the gut barrier, thereby impeding the distribution of bacteria and toxins (15). Microbial regulation is pertinent to maintaining the homeostasis of the gut-liver axis, as it plays an important role in sustaining the microbial communities within the intestine.

A certain number of toxicological studies have looked at the impact of dioxin-like PCBs on the gut microbiome. Specifically, PCB 126 increased the Firmicutes:Bacteroidetes ratio; decreased the intestinal bacterial diversity and decreased organokines, such as glucagon peptide 1 (GLP-1) (16, 17). PCB 126 reduction in gut diversity was associated with fifteen different NAFLD biomarkers, such as hepatic inflammation, steatosis, and metabolism (17). Exposure to another dioxin-like PCB,

namely PCB 77, also led to increased Firmicutes:Bacteroidetes ratio, as well as serum bile acids, hepatic steatosis, inflammation, and fibrosis (18). In addition, studies investigating non-dioxin-like PCBs and their impact on the gut microbiome have also reported that Aroclor 1260 exposure led to altered alpha and beta diversity in mouse models (9). A unique aspect of our current study is that we are assessing the impact of a mixture of PCBs that consist of both dioxin-like and non-dioxin-like congeners and is therefore, more environmentally relevant, since people are exposed to both classes.

Our results thus far indicate that there were significant microbiome alterations regarding the alpha diversity, based on sex and PCB exposure. Importantly, the alpha diversity findings showed that the PCB-exposed female group had the lowest diversity, implicating that PCB exposure in the female mice drastically reduced the bacterial variety. According to reported literature, a decrease in alpha diversity is often associated with unhealthy conditions or diseased states including obesity and NAFLD (19). Indeed, in our study, when we were investigating liver end points in this model, we observed that the PCB-exposed female mice have more exacerbated hepatic injury, inflammation, and steatosis. This, in part, validated our hypothesis that there is an interaction between the gut and liver, driving these sex-dependent toxicities with PCB exposure. With regard to beta diversity, there were also observable sex differences, as both males and females behave differently in terms of gut microbiome and the addition of PCB exposure exacerbated the difference reported in beta diversity.

Through the assessment of the gut barrier functions and inflammation using RT-PCR, we discovered that certain gut barrier markers were altered with PCB exposure, and this effect was more predominant in PCB-exposed female mice. Indeed, the gene

expression for the gut barrier proteins, namely Mucin 2 and Occludin, were decreased in the exposed female group. Mucin 2 forms the skeleton of the intestinal mucus and covers and protects the intestinal tract from self-digestion and numerous microorganisms (20) while occludin plays an integral role in the maintenance of tight junction assembly (21). Surprisingly, Claudin-2, which is expressed in the tight junctions of leaky epithelia (22), was also decreased in the exposed female group. Nonetheless, the results demonstrated a difference in gene expression for proteins that regulate gut barrier function and this needs to be further investigated.

In the current study, there were no significant differences observed in inflammatory markers. A potential reason for this could be the short-term duration of PCB exposure in the current study. We hypothesized that a longer duration of exposure would lead to a pro-inflammatory state in the PCB-exposed females. However, PCB-exposed females did exhibit lower mRNA levels of *Tff3,* the gene encoding the antimicrobial peptide TFF3. Intestinal *Tff3* was recently demonstrated to play an important role in reducing gut permeability, and alleviating liver damage and administering *Tff3* is potentially considered a therapeutic strategy for non-alcoholic steatohepatitis (23).

The overall results so far are in concordance with our previously reported sex-dependent PCB effects where we demonstrated that female mice were more susceptible to PCB-mediated liver injury. The current results suggest that a potential mechanism that may explain the observed liver outcomes is due to female mice acquiring a different microbial profile than males. Additional analyses of the particular phyla influencing these differences will be further evaluated. Another potential mechanism that will require further elucidation is how the different bacteria crosstalk with PCB receptors such as AhR and

CAR. Hepatic proteomic measurements were previously performed for this study (data not shown), and the analysis revealed that PCB-exposed female mice had higher protein levels of the AhR targets, namely flavin monooxygenases (FMOs). It is well-known that one of the FMOs, namely FMO3, has an important relationship with the gut microbiome in metabolizing the food derivative trimethylamine to trimethyl amine N-oxide (TMAO) (24, 25). Increased levels of TMAO have been associated with metabolic dysfunction in cardiovascular disease (26). The role of the AhR, gut microbiome and metabolic and hepatic dysfunction in female mice warrant further investigation. Moreover, our research group has previously shown that PCB interactions with hepatic nuclear receptors such as CAR and PXR also drive gut microbiome changes in diet-induced obese male mice (9). These interactions will also be evaluated in the current study using integrated proteomics-metagenomics analyses.

CONCLUSION

To summarize, our results thus far indicate that sex played a significant role in dictating PCB-induced gut microbiome alterations. Additionally, examination of ileal gene expression provided further evidence that PCB effects on gut barrier properties were sex-dependent, given that female mice were more susceptible to these PCB-induced effects. While the study is highly novel as it is one of the first studies to examine sex differences in gut microbiome with PCB exposures, it is however not without limitations. The exposure study was acute in nature, and does not reflect long-term exposures that occur in humans today. Also, estrus cycle in female mice was not monitored over the study period. Importantly, the results so far do not provide information on the bacterial taxa that were altered with sex and exposure. These concerns will be addressed in our future studies. Nonetheless, the current study highlighted how sex differences play a role in dictating toxicity endpoints caused by environmental toxicant exposures. Further studies correlating bacterial abundance with liver disease endpoints will provide more knowledge on how the disrupted gut-liver axis drives PCB toxicity in female mice.

SIGNIFICANCE AND IMPACT

The findings from our current project will help in better understanding PCB effects on the relationship between the liver and the gut microbiota (gut-liver axis), and how these effects can be identified in PCB-exposed populations. Based on previous studies, we have demonstrated that PCBs can contribute to fatty liver disease, and it is well-known that there is a cross interaction between the liver and the microbiome in the gut. Therefore, our studies will provide a more complete understanding of how PCBs can impact the interaction between the liver and the gut. The findings on sex differences will also help in better risk assessment of populations that may be more susceptible to PCB-induced toxicity and will better address knowledge gaps in health disparities related to environmental pollution. Our study objective and findings are relevant to PCB-exposed populations such as the ACHS cohort and others.

FUTURE DIRECTIONS

We will be examining bacterial abundance within samples to identify bacterial phyla that play a role in driving the observed PCB effects dependent on sex. In addition, we will further explore studies looking at long-term effects of PCB exposure on gut microbiome and gut-liver axis, and how high caloric diets such as high fat diet can influence PCB-mediated effects. Specifically, we will investigate whether these findings will translate to human exposures using our available human epidemiological data.

ACKNOWLEDGEMENTS

I would like to acknowledge the UofL Genomics Facility, which is supported, in part, by NIH P20GM103436 (KY IDeA Networks of Biomedical Research Excellence), the UofL J. G. Brown Cancer Center, the UofL Department of Medicine, Division of Hepatology, Gastroenterology and Nutrition, the TriBeta Research Foundation, and the UofL Center for Integrative Environmental Health Sciences (CIEHS) Research Voucher Program. I would also like to acknowledge the Cave and Wahlang Lab members, as well as Dr. Richa Singhal.

REFERENCES

1. Kimbrough RD. Polychlorinated biphenyls (PCBs) and human health: an update. Crit Rev Toxicol. 1995;25(2):133-63. Epub 1995/01/01. doi: 10.3109/10408449509021611. PubMed PMID: 7612174.
2. Wahlang B, Falkner KC, Clair HB, Al-Eryani L, Prough RA, States JC, Coslo DM, Omiecinski CJ, Cave MC. Human receptor activation by aroclor 1260, a polychlorinated biphenyl mixture. Toxicol Sci. 2014;140(2):283-97. Epub 2014/05/09. doi: 10.1093/toxsci/kfu083. PubMed PMID: 24812009; PMCID: PMC4176050.
3. Jin J, Wahlang B, Shi H, Hardesty JE, Falkner KC, Head KZ, Srivastava S, Merchant ML, Rai SN, Cave MC, Prough RA. Dioxin-like and non-dioxin-like PCBs differentially regulate the hepatic proteome and modify diet-induced nonalcoholic fatty liver disease severity. Med Chem Res. 2020;29:1247-63. Epub 2020/08/25. doi: 10.1007/s00044-020-02581-w. PubMed PMID: 32831531; PMCID: PMC7440142.
4. Wahlang B, Song M, Beier JI, Cameron Falkner K, Al-Eryani L, Clair HB, Prough RA, Osborne TS, Malarkey DE, States JC, Cave MC. Evaluation of Aroclor 1260 exposure in a mouse model of diet-induced obesity and non-alcoholic fatty liver disease. Toxicol Appl Pharmacol. 2014;279(3):380-90. Epub 2014/07/08. doi: 10.1016/j.taap.2014.06.019. PubMed PMID: 24998970; PMCID: PMC4225625.
5. Wahlang B, Beier JI, Clair HB, Bellis-Jones HJ, Falkner KC, McClain CJ, Cave MC. Toxicant-associated steatohepatitis. Toxicol Pathol. 2013;41(2):343-60. Epub

2012/12/25. doi: 10.1177/0192623312468517. PubMed PMID: 23262638; PMCID: PMC5114851.

6. Clair HB, Pinkston CM, Rai SN, Pavuk M, Dutton ND, Brock GN, Prough RA, Falkner KC, McClain CJ, Cave MC. Liver Disease in a Residential Cohort With Elevated Polychlorinated Biphenyl Exposures. Toxicol Sci. 2018;164(1):39-49. Epub 2018/04/24. doi: 10.1093/toxsci/kfy076. PubMed PMID: 29684222; PMCID: PMC6016643.

7. Wahlang B, Jin J, Hardesty JE, Head KZ, Shi H, Falkner KC, Prough RA, Klinge CM, Cave MC. Identifying sex differences arising from polychlorinated biphenyl exposures in toxicant-associated liver disease. Food Chem Toxicol. 2019;129:64-76. Epub 2019/04/27. doi: 10.1016/j.fct.2019.04.007. PubMed PMID: 31026535; PMCID: PMC6555661.

8. Kakizaki S, Yamazaki Y, Takizawa D, Negishi M. New insights on the xenobiotic-sensing nuclear receptors in liver diseases--CAR and PXR. Curr Drug Metab. 2008;9(7):614-21. Epub 2008/09/11. doi: 10.2174/138920008785821666. PubMed PMID: 18781913.

9. Wahlang B, Alexander NC, 2nd, Li X, Rouchka EC, Kirpich IA, Cave MC. Polychlorinated biphenyls altered gut microbiome in CAR and PXR knockout mice exhibiting toxicant-associated steatohepatitis. Toxicol Rep. 2021;8:536-47. Epub 2021/03/30. doi: 10.1016/j.toxrep.2021.03.010. PubMed PMID: 33777700; PMCID: PMC7985695.

10. Wahlang B, Jin J, Beier JI, Hardesty JE, Daly EF, Schnegelberger RD, Falkner KC, Prough RA, Kirpich IA, Cave MC. Mechanisms of Environmental Contributions

to Fatty Liver Disease. Curr Environ Health Rep. 2019;6(3):80-94. Epub 2019/05/28. doi: 10.1007/s40572-019-00232-w. PubMed PMID: 31134516; PMCID: PMC6698418.

11. Livak KJ, Schmittgen TD. Analysis of relative gene expression data using real-time quantitative PCR and the 2(-Delta Delta C(T)) Method. Methods. 2001;25(4):402-8. Epub 2002/02/16. doi: 10.1006/meth.2001.1262. PubMed PMID: 11846609.

12. Zhang L, Wang YD, Chen WD, Wang X, Lou G, Liu N, Lin M, Forman BM, Huang W. Promotion of liver regeneration/repair by farnesoid X receptor in both liver and intestine in mice. Hepatology. 2012;56(6):2336-43. Epub 2012/06/20. doi: 10.1002/hep.25905. PubMed PMID: 22711662; PMCID: PMC3477501.

13. Larsson E, Tremaroli V, Lee YS, Koren O, Nookaew I, Fricker A, Nielsen J, Ley RE, Backhed F. Analysis of gut microbial regulation of host gene expression along the length of the gut and regulation of gut microbial ecology through MyD88. Gut. 2012;61(8):1124-31. Epub 2011/11/26. doi: 10.1136/gutjnl-2011-301104. PubMed PMID: 22115825; PMCID: PMC3388726.

14. Hartmann P, Hochrath K, Horvath A, Chen P, Seebauer CT, Llorente C, Wang L, Alnouti Y, Fouts DE, Starkel P, Loomba R, Coulter S, Liddle C, Yu RT, Ling L, Rossi SJ, DePaoli AM, Downes M, Evans RM, Brenner DA, Schnabl B. Modulation of the intestinal bile acid/farnesoid X receptor/fibroblast growth factor 15 axis improves alcoholic liver disease in mice. Hepatology. 2018;67(6):2150-66. Epub 2017/11/22. doi: 10.1002/hep.29676. PubMed PMID: 29159825; PMCID: PMC5962369.

15. Albillos A, de Gottardi A, Rescigno M. The gut-liver axis in liver disease: Pathophysiological basis for therapy. J Hepatol. 2020;72(3):558-77. Epub 2019/10/18. doi: 10.1016/j.jhep.2019.10.003. PubMed PMID: 31622696.

16. Petriello MC, Hoffman JB, Vsevolozhskaya O, Morris AJ, Hennig B. Dioxin-like PCB 126 increases intestinal inflammation and disrupts gut microbiota and metabolic homeostasis. Environ Pollut. 2018;242(Pt A):1022-32. Epub 2018/10/31. doi: 10.1016/j.envpol.2018.07.039. PubMed PMID: 30373033; PMCID: PMC6211811.

17. Chi Y, Lin Y, Lu Y, Huang Q, Ye G, Dong S. Gut microbiota dysbiosis correlates with a low-dose PCB126-induced dyslipidemia and non-alcoholic fatty liver disease. Sci Total Environ. 2019;653:274-82. Epub 2018/11/10. doi: 10.1016/j.scitotenv.2018.10.387. PubMed PMID: 30412872.

18. Chi Y, Wang H, Lin Y, Lu Y, Huang Q, Ye G, Dong S. Gut microbiota characterization and lipid metabolism disorder found in PCB77-treated female mice. Toxicology. 2019;420:11-20. Epub 2019/04/03. doi: 10.1016/j.tox.2019.03.011. PubMed PMID: 30935970.

19. Del Chierico F, Nobili V, Vernocchi P, Russo A, De Stefanis C, Gnani D, Furlanello C, Zandona A, Paci P, Capuani G, Dallapiccola B, Miccheli A, Alisi A, Putignani L. Gut microbiota profiling of pediatric nonalcoholic fatty liver disease and obese patients unveiled by an integrated meta-omics-based approach. Hepatology. 2017;65(2):451-64. Epub 2016/03/31. doi: 10.1002/hep.28572. PubMed PMID: 27028797.

20. Pelaseyed T, Bergstrom JH, Gustafsson JK, Ermund A, Birchenough GM, Schutte A, van der Post S, Svensson F, Rodriguez-Pineiro AM, Nystrom EE, Wising C, Johansson ME, Hansson GC. The mucus and mucins of the goblet cells and enterocytes provide the first defense line of the gastrointestinal tract and interact with the immune system. Immunol Rev. 2014;260(1):8-20. Epub 2014/06/20. doi: 10.1111/imr.12182. PubMed PMID: 24942678; PMCID: PMC4281373.

21. Rao R. Occludin phosphorylation in regulation of epithelial tight junctions. Ann N Y Acad Sci. 2009;1165:62-8. Epub 2009/06/23. doi: 10.1111/j.1749-6632.2009.04054.x. PubMed PMID: 19538289; PMCID: PMC6202026.

22. Matsumoto K, Imasato M, Yamazaki Y, Tanaka H, Watanabe M, Eguchi H, Nagano H, Hikita H, Tatsumi T, Takehara T, Tamura A, Tsukita S. Claudin 2 deficiency reduces bile flow and increases susceptibility to cholesterol gallstone disease in mice. Gastroenterology. 2014;147(5):1134-45 e10. Epub 2014/07/30. doi: 10.1053/j.gastro.2014.07.033. PubMed PMID: 25068494.

23. Wang Y, Liang K, Kong W. Intestinal Trefoil Factor 3 Alleviates the Intestinal Barrier Function Through Reducing the Expression of TLR4 in Rats with Nonalcoholic Steatohepatitis. Arch Med Res. 2019;50(1):2-9. Epub 2019/05/19. doi: 10.1016/j.arcmed.2019.03.004. PubMed PMID: 31101239.

24. Rowland I, Gibson G, Heinken A, Scott K, Swann J, Thiele I, Tuohy K. Gut microbiota functions: metabolism of nutrients and other food components. Eur J Nutr. 2018;57(1):1-24. Epub 2017/04/11. doi: 10.1007/s00394-017-1445-8. PubMed PMID: 28393285; PMCID: PMC5847071.

25. Fennema D, Phillips IR, Shephard EA. Trimethylamine and Trimethylamine N-Oxide, a Flavin-Containing Monooxygenase 3 (FMO3)-Mediated Host-Microbiome Metabolic Axis Implicated in Health and Disease. Drug Metab Dispos. 2016;44(11):1839-50. Epub 2016/10/21. doi: 10.1124/dmd.116.070615. PubMed PMID: 27190056; PMCID: PMC5074467.

26. Schoeler M, Caesar R. Dietary lipids, gut microbiota and lipid metabolism. Rev Endocr Metab Disord. 2019;20(4):461-72. Epub 2019/11/11. doi: 10.1007/s11154-019-09512-0. PubMed PMID: 31707624; PMCID: PMC6938793.